UNIVERSITY OF BIRMINGHAM

Effect of wavefront aberrations on a focused plenoptic imaging system: a wave optics simulation approach

Turola, Massimo; Meah, Christopher; Marshall, Richard J.; Styles, Iain B.; Gruppetta, Steve

Document Version
Publisher's PDF, also known as Version of record

Link to publication on Research at Birmingham portal

Effect of wavefront aberrations on a focused plenoptic imaging system; a wave optics simulation approach

Massimo Turola[a], Chris J. Meah[b], Richard J. Marshall[b], Iain B. Styles[bc] and Stephen Gruppetta[a]

[a]Centre for Applied Vision Research, School of Health Sciences, City University London, London, UK;
[b]PSIBS Doctoral Training Centre, School of Chemistry, University of Birmingham, Edgbaston, UK
[c]School of Computer Science, University of Birmingham, Edgbaston, UK

ABSTRACT

A plenoptic imaging system records simultaneously the intensity and the direction of the rays of light. This additional information allows many post processing features such as 3D imaging, synthetic refocusing and potentially evaluation of wavefront aberrations. In this paper the effects of low order aberrations on a simple plenoptic imaging system have been investigated using a wave optics simulations approach.

Keywords: Plenoptic imaging, wavefront sensor, aberrations, numerical simulations

1. INTRODUCTION

A plenoptic imaging system records the light field, which is a four dimensional function, also known as the plenoptic function, describing radiance along rays as a function of position and direction.[1] The light field is recorded by adding a lenslet array in front of the sensor plane of the camera as shown in figure 1. A raw plenoptic image consists of an array of lenslet sub-images, corresponding to different point of views. The final image is then rendered as explained by Georgiev *etal.*.[2] An example of a raw image is shown in figure 2. The information encoded in a plentoptic image can be computationally post-processed for synthetic refocusing, 3D depth mapping, tomography, and potentially the evaluation of wavefront aberrations. According to geometric optics, ray directions are defined by the wave vectors **k** that describe a set of vectors perpendicular to the surfaces of constant phase of the wavefront. Aberrations are deviations from an ideal spherical reference wavefront and thus in an aberrated optical system the rays, in general, do not strike the focal plane at positions that correspond to the paraxial (ideal) image location.[3] We consider the behaviour of a focused plenoptic camera in the presence of different wavefront aberrations. Deviations in ray directions that result from aberrations will produce a shift in each lenslet sub-image with respect to the ideal sub-image, and therefore the distribution and magnitude of the sub-image displacements gives an estimation of the aberrations in the system. We use a wave optics approach to more simulate image formation in a plenoptic camera in the presence of aberrations.

2. METHOD

Numerical simulations of light propagation in a focused plenoptic imaging system have been performed in MAT-LAB. The imaging system is modelled as a combination of two simple transformations: free space propagation and passage through a lens.[4] Free space propagation is simulated using the angular spectrum of plane waves method. The optical field at the object plane $U(x, y; 0)$ is decomposed as a sum of plane waves with different spatial frequencies f_x and f_y, defined as the angular spectrum $A(f_x, f_y; 0)$, as shown in equation 1. The angular
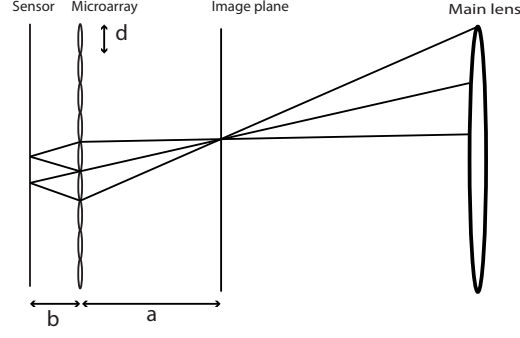
Figure 1. Diagram of a focused plenoptic imaging system. The main lens is in a 2f configuration. The lenslet array satisfies the lens equation between the main lens image and the sensor plane. d is the pitch of the lenslet
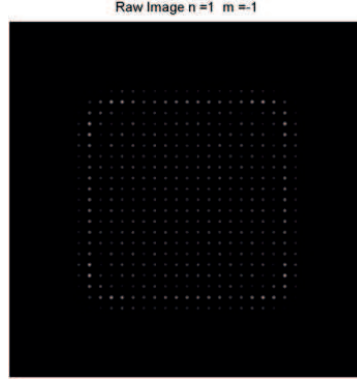

Figure 2. Raw plenoptic image of a monochromatic plane wave as it appears on the sensor plane. Each lenslet creates an elemental sub image corresponding to a different point of view.

spectrum after the propagation is given by equation 2. The propagation can be treated as a linear filter whose transfer function H has a finite bandwidth that depends on the propagation distance z (equation 3).[4]

$$A(f_x, f_y; 0) = \iint_{-\infty}^{+\infty} U(x, y; 0)e^{i2\pi(f_x x + f_y y)}\mathrm{d}x\mathrm{d}y \tag{1}$$

$$A(f_x, f_y; z) = A(f_x, f_y; 0)H(f_x, f_y), \tag{2}$$

$$H(f_x, f_y) = \begin{cases} e^{ikz\sqrt{1-(\lambda f_x)^2-(\lambda f_y)^2}} & \sqrt{(f_x)^2 + (f_y)^2} < \frac{1}{\lambda} \\ 0 & elsewhere \end{cases} \tag{3}$$

Optical elements such as a thin lens with focal length f and lenslet arrays are simulated as a circular pupil $P(x, y)$, or an array of pupils, with a quadratic phase factor

$$L(x, y) = P(x, y)e^{i\frac{k}{2f}(x^2+y^2)}. \tag{4}$$

Aliasing arising from the digital sampling of the transfer function is treated using the band-limited angular spectrum method.[5] Similar considerations can be made to treat lens phase profile aliasing.[6] Wavefront aberrations are modeled by adding a phase mask to the main lens such that

$$\tilde{P}(x, y) = P(x, y)e^{ikW(x,y)}, \tag{5}$$

where $W(x, y)$ is the aberration function. Switching to polar coordinates, the aberration function $W(\rho, \theta)$ can be expressed as a linear combination of polynomials orthogonal on the unit circle:

$$W(\rho, \theta) = \sum_{m=0, n=0}^{\infty} C_n^m Z_n^m(\rho, \theta). \tag{6}$$

where C_n^m gives the magnitude of the aberrations and $Z_n^m(\rho, \theta)$ are the Zernike polynomials. n and m define the order of the aberration.

3. SIMULATIONS

The simulated system (figure 1) consists of a main lens of focal length 120mm in a 2f configuration. The microlens array consists of 35×35 lenslets of focal length 8 mm and pitch of 143 μm, placed at distance a from the main lens image plane and b from the sensor plane respectively in order to satisfy the lens equation $1/f = 1/a + 1/b$. a and b are respectively 32mm and 10.7 mm. Magnification was $m = b/a = 0.33$.

After acquiring the non-aberrated raw image of a plane wave, low order aberrations were added on the main lens pupil. The shifts of each sub-image in the raw image have been estimated by cross correlating each sub-image with the sub-image in the same position in the ideal raw image. These values arranged in an array tell how much each sub-image is shifted because of aberrations.

4. RESULTS

Figure 3 shows maps of the vectors of displacement map for a raw image of a plane wave, after the addition of a number of types of aberration. The aberrations added to the main lens are: vertical and horizontal tilt ($n = 1, m = -1$ and $n = 1, m = 1$), astigmatism ($n = 2, m = -2$ and $n = 2, m = 2$) and coma ($n = 3, m = -1$ and $n = 3, m = 1$). For all these aberrations the C_n^m coefficient is 0.1 mum. For clarity reasons the shift vectors has been scaled by a factor of 2. Results of the simulations with high order aberrations have not been included in this abstract for brevity. In figure 4 are represented the aberrations functions added to the main lens.

5. CONCLUSIONS AND FUTURE WORK

This work has shown the effect that simple low order aberrations have on raw plenoptic images. Cross-correlating aberrated sub-images with the ideal case allows a displacement map can be generated. This information could be used in several ways, for example, through the creation of a library of displacement maps to be used during the calibration of plenoptic cameras in presence of aberrations. With a reverse ray tracing algorithm from the generated raw images,[7] it should be possible to estimate the wavefront at any point during the propagation, converting a plenoptic camera into a wavefront sensor. The sensitivity of raw images to wavefront aberrations could be used to develop an imaging system capable of capturing intensity and phase information at the same time.

REFERENCES

[1] Levoy, M., Zhang, Z., and McDowall, I., "Recording and controlling the 4d light field in a microscope using microlens arrays," *Journal of microscopy* **235**(2), 144–162 (2009).

[2] Georgiev, T. and Lumsdaine, A., "Focused plenoptic camera and rendering," *Journal of Electronic Imaging* **19**(2), 021106–021106 (2010).

[3] Sinzinger, S. and Jahns, J., [*Microoptics*], Wiley Online Library (2003).

[4] Goodman, J., [*Introduction to Fourier optics*], McGraw-hill (2008).

[5] Matsushima, K. and Shimobaba, T., "Band-limited angular spectrum method for numerical simulation of free-space propagation in far and near fields," *Optics express* **17**(22), 19662–19673 (2009).

[6] Turola, M. and Gruppetta, S., "Wave optics simulations of a focused plenoptic system," in [*Laser Science*], JTu3A–24, Optical Society of America (2014).

[7] Schwiegerling, J., "Plenoptic camera image simulation for reconstruction algorithm verification," in [*SPIE Optical Engineering+ Applications*], 91930V–91930V, International Society for Optics and Photonics (2014).
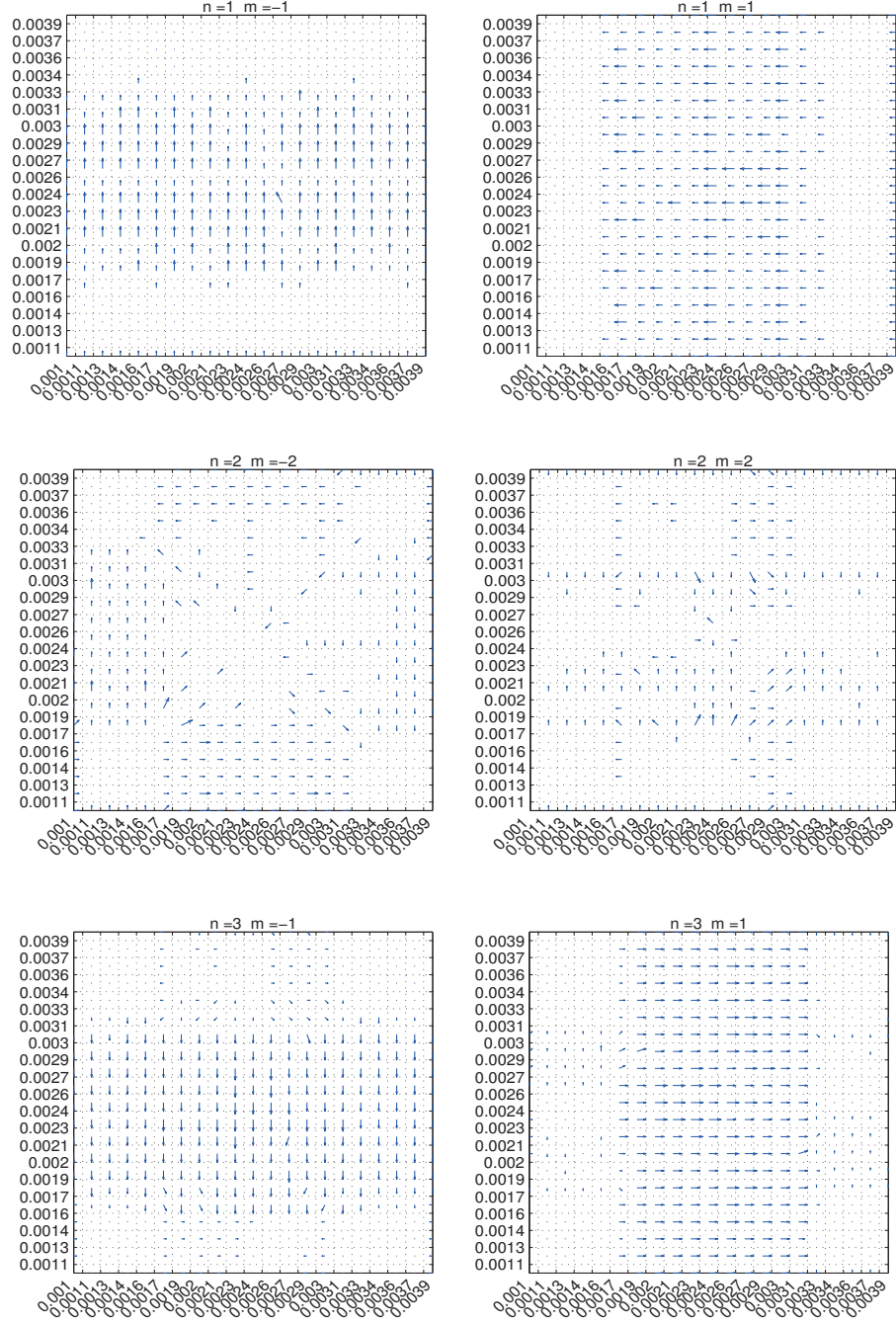
Figure 3. Displacements distibution for raw images of a monochromatic plane wave following the addition of aberrations. The pattern is seen to vary according to the type of aberration. From top left to bottom right: tilt ($n = 1, m = -1$ and $n = 1, m = 1$), astigmatism ($n = 2, m = -2$ and $n = 2, m = 2$) and coma, ($n = 3, m = -1$ and $n = 3, m = 1$). Array size: $5mm$, each square on the grid represents a sub-image, dimension of the sub-images in meters are shown on the axis. Shift vectors has been scaled of a factor 2 for representing clearer data.
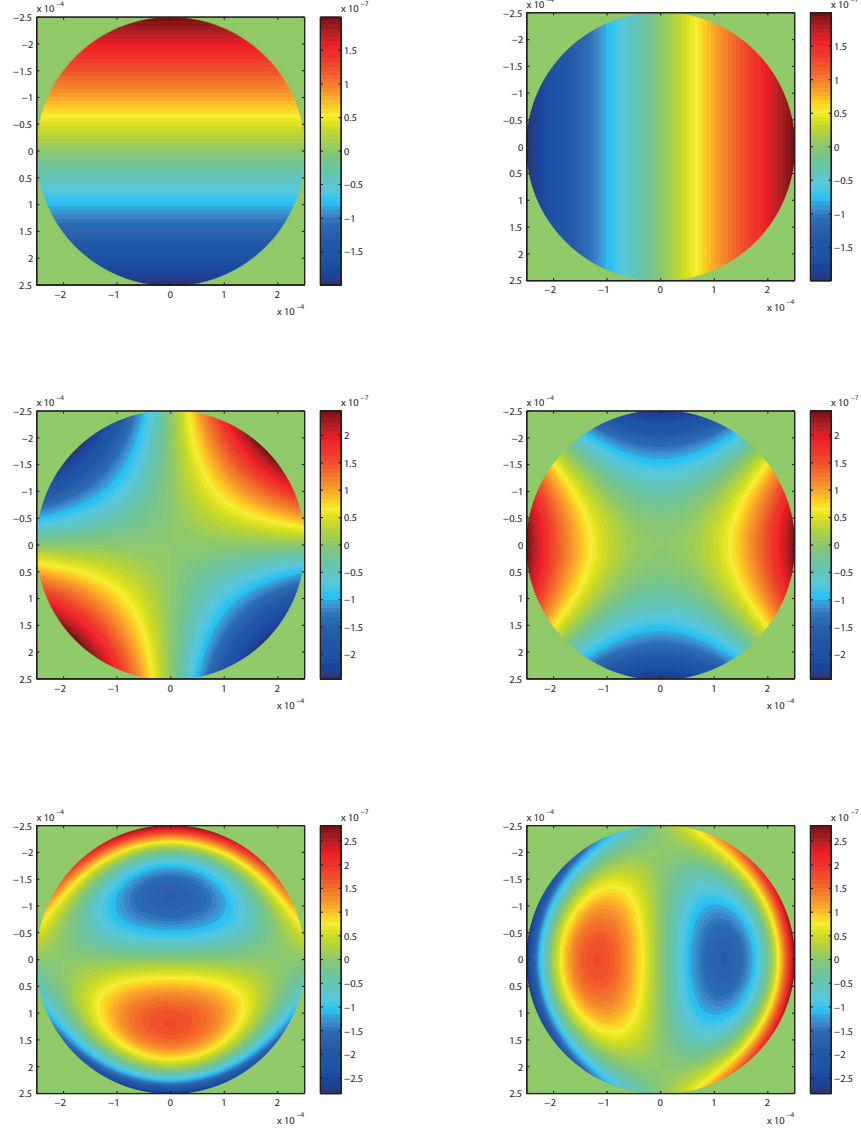
Figure 4. Wavefront aberration functions added to the optical fields at the main lens pupil plane. From top left: tilt $(n = 1, m = -1$ and $n = 1, m = 1)$, astigmatism $(n = 2, m = -2$ and $n = 2, m = 2)$ and coma, $(n = 3, m = -1$ and $n = 3, m = 1)$. Colorbar indicates the amplitude of the deviation from the spherical wavefront in meters.